# Occupation at Carpenters Gap 3,

## Windjana Gorge, Kimberley, Western Australia

*Sue O'Connor[1], Tim Maloney[1], Dorcas Vannieuwenhuyse[2], Jane Balme[2] and Rachel Wood[3]*

[1] Archaeology and Natural History, College of Asia and the Pacific, The Australian National University, Canberra ACT 0200, Australia <sue.oconnor@anu.edu.au> <tim.maloney@anu.edu.au>

[2] Archaeology, School of Social Sciences, The University of Western Australia, 35 Stirling Highway, Crawley WA 6009, Australia <dorcas.vannieuwenhuyse@research.uwa.edu.au> <jane.balme@uwa.edu.au>

[3] Radiocarbon Facility, Research School of Earth Sciences, College of Physical and Mathematical Science, The Australian National University, Canberra ACT 0200, Australia <rachel.wood@anu.edu.au>

***Abstract***

*Carpenters Gap 3 (CG3), a limestone cave and shelter complex in the Napier Range, Western Australia, was occupied by Aboriginal people intermittently from over 30,000 years ago through to the historic period. Excavations at CG3 provide only slight evidence for occupation following first settlement in the late Pleistocene. Analysis of the radiocarbon dates indicates that following this there was a hiatus in occupation during the Last Glacial Maximum. In common with most Australian sites, the evidence for occupation increases sharply from the mid-Holocene. Faunal remains, interpreted predominantly as the remains of people's meals, all suggest foraging of the immediate surroundings throughout the entire period of occupation. Fragments of baler shell and scaphopod beads are present from the early Holocene, suggesting movement of high value goods from the coast (over 200 km distant). Flakes from edge-ground axes recovered from occupation units dated to approximately 33,000 cal. BP, when overall artefact numbers are low, suggest that these tools formed an important component of the lithic repertoire at this time.*

### Introduction

Carpenters Gap 3 (CG3) is a limestone cave and overhang complex in the Napier Range, southern Kimberley, Western Australia (WA) (Figure 1). It is located on the north side of the range, a few hundred metres east of the Lennard River, where it cuts through the range forming Windjana Gorge. CG3 includes an extensive overhang about 30 m above the plain containing a spectacular gallery of painted art, and a lower cave—which appears to have been formed by solution—that extends at least 30 m into the range. The floor of the overhang has extensive evidence of human occupation, such as in situ ground and incised surfaces, stone artefacts and freshwater mussel shell valves, but contains only small pockets of sediment with little excavation potential and in places the floor comprises bare rock. The main deposit at CG3 is found within the lower cave which, in places, shows extensive surface cracking, indicating that it is subject to seasonal or periodic wetting and drying. No cultural material was visible on this relatively level surface.

CG3 was first excavated by O'Connor in 1993 as part of a regional archaeological investigation programme, at which time a 1 m square (Pit A) was excavated about 17 m inside the drip-line within the lower cave (Figure 2). Pit A was excavated to a maximum depth of 168 cm without reaching bedrock (Figure 3), at which time excavation was discontinued and the pit was backfilled. Radiocarbon age estimates obtained on charcoal, seeds and freshwater shell demonstrated occupation spanning over 30,000 years and, although since incorporated into regional syntheses (e.g. O'Connor and Veth 2006:36), neither the CG3 dates nor details of the excavation were ever fully reported. In August 2012 we returned to CG3 in order to extend Pit A, including for the purposes of reaching bedrock. The original pit was emptied and the excavation was continued to a maximum depth of 2.4 m, where bedrock was encountered (Figures 3 and 4). Here we present the full suite of radiocarbon dates and finds from CG3 Pit A from both the 1993 and 2012 field seasons.

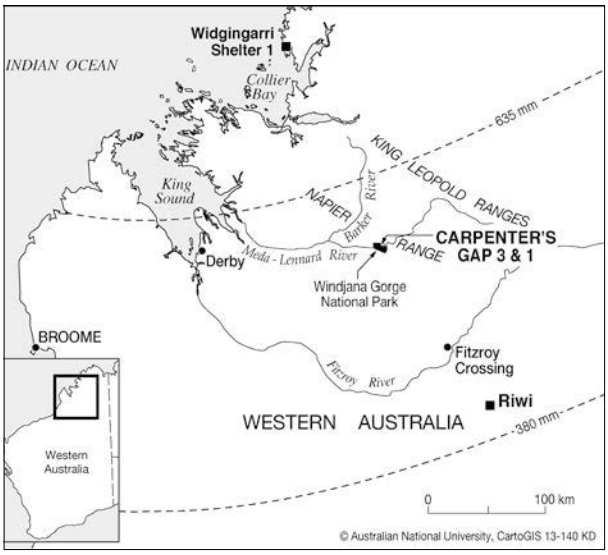


**Figure 1** Location of CG3 in Windjana Gorge National Park and other sites mentioned in the text.

## Excavation and Recovery at CG3: The 1993 and 2012 Field Seasons

The 1993 excavation was carried out in 2–5 cm excavation units (spits). In the upper part of the deposit, excavation units (XUs) averaged 3 cm, whereas in the lower deposits excavated in 1993, as well as those during the 2012 field season, and in which little or no cultural material was encountered, XU thicknesses were greater. This is reflected clearly in the volumes of excavated sediment (Figure 3). The stratigraphic layers sloped towards the southeast corner of the excavation, with a slope gradient decreasing from bottom to top. Owing to the difficulty in identifying stratigraphic changes during excavation, XUs were horizontal, resulting in some cross-cutting stratigraphic layers (Figure 3). All excavated materials were dry sieved on-site through nested 6 and 3 mm sieves during the 1993 field season, and 5 and 1.5 mm sieves during the 2012 season. All dated organic material was recovered from the sieve residues.

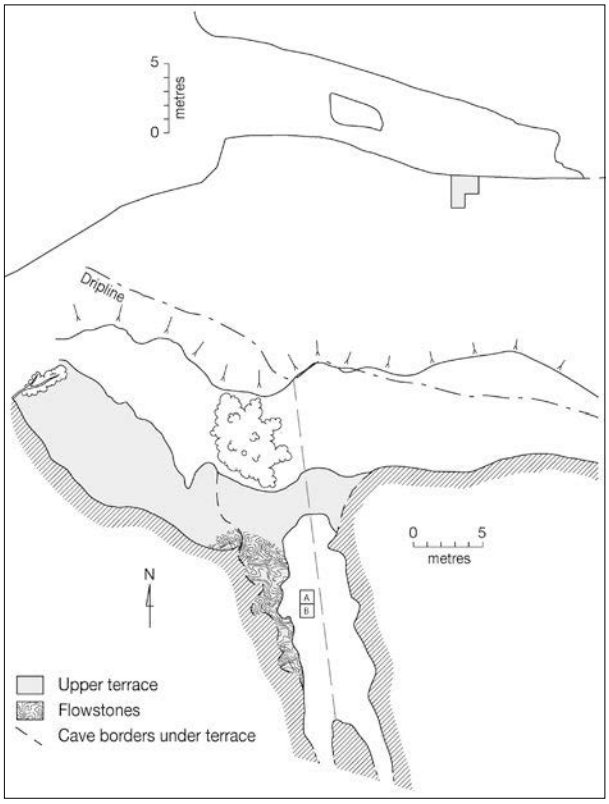


**Figure 2** CG3 cross-section (top) and site plan (bottom) showing cave, overhang, and 1993 and 2012 excavations.

## CG3 Sediments and Depositional Processes

The CG3 sediments are relatively homogeneous, primarily brown (7.5YR4/4), though close inspection reveals some subtle colour differences (Figure 4). Texturally, the sediment is fine sandy silt in the upper part of the deposit (Stratigraphic Layers 1–11), becoming increasingly sandier below Layer 12. Loose gravels and rocks occur throughout. The sand fraction is primarily composed of quartz, though mica particles also occur through the profile in various proportions. All the sediment components seem to derive from the surrounding parent material of complex bedded limestone and sandstone, and have accumulated via run-off, aeolian or mechanical means. The cave's entrance is steeply sloped and this would have facilitated the movement of materials and sediments from the upper terrace into the lower cave. The enclosed character of the lower cave has worked as a natural trap for sediment, resulting in a greater accumulation of sediments than other excavated sites in the area (e.g. O'Connor 1995).

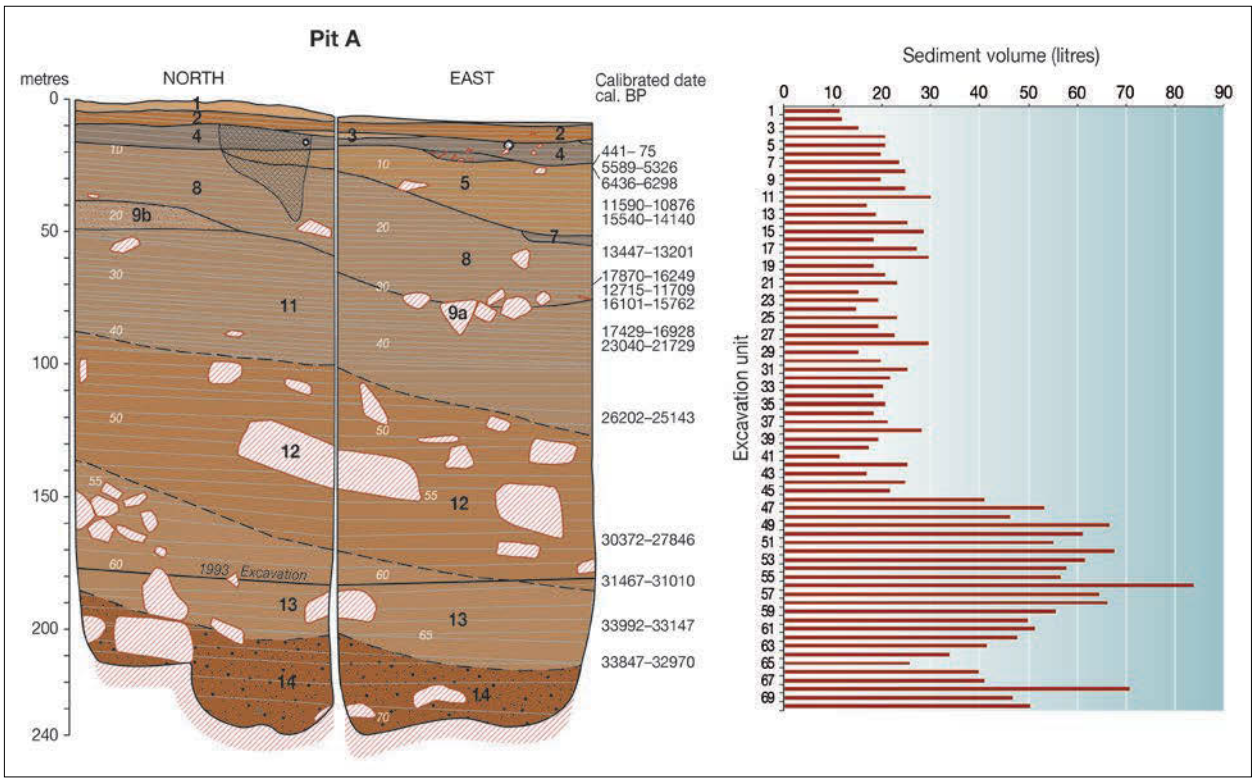


**Figure 3** Profile of CG3 excavation Square A, showing XU depths as they relate to stratigraphic layers, depth of 1993 excavation and volume of sediment removed for each XU.

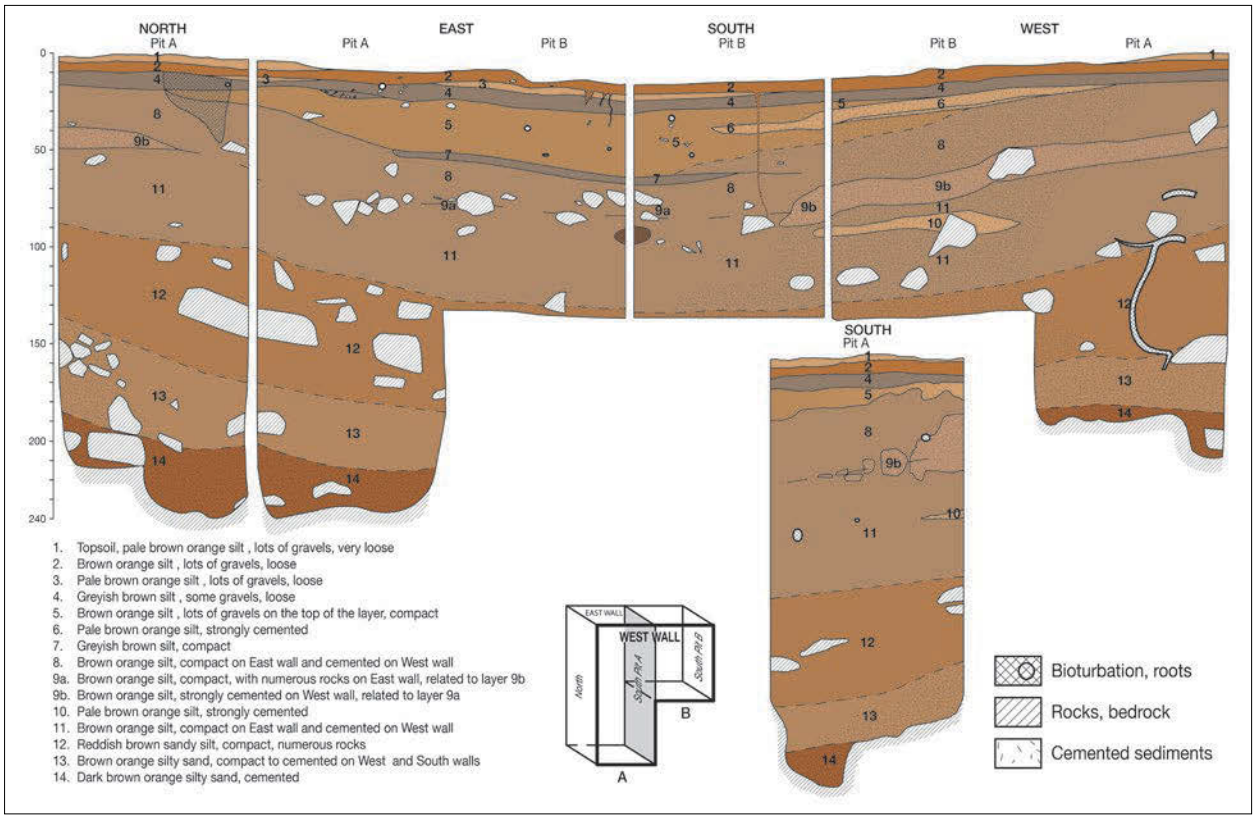


**Figure 4** CG3 stratigraphic profiles of Pits A (1993) and B (2012).

Three major depositional strata can be distinguished in the deposit (Figure 4). The first includes Layers 14–12 (sediments of a sandy silt texture with large limestone cobbles), which corresponds to the initial accumulation episode in the cave. The second, comprising Layers 11–8, is a homogeneous, thick accumulation, except for Layer 9. The latter is represented on the east wall by rock fall (Layer 9a) and on the west wall as a carbonate cemented layer (Layer 9b). The latter may indicate a phase of wetter conditions where more water was entering or pooling in the cave. The last stratum (Layers 7–1) consists of several thin laminated layers, of which Layers 7 and 4 are greyer than the others, possibly due to larger amounts of organic matter and/or the presence of small charcoal particles. Future micromorphological and geochemical analyses may help determine whether these differences are related to increased anthropogenic activity or other causes.

Thick roots have penetrated through the sediment into the deeper layers, where moisture seems to be present all year long. Bioturbation, in the form of insect channels and small roots, is also visible in the upper layers. Processes resulting in the dissolution and precipitation of calcium carbonate have taken place throughout the history of the cave and have differentially affected the deposit. This is particularly evident in the western side of the deposit, which is heavily cemented below Layer 4. Speleothems and flowstones are present in both the cave and shelter, and are still actively forming during the wet season.

Owing to the high carbonate content in the sediments the pH is uniformly 8.5 (alkaline) throughout. Consequently, preservation is excellent, although organic cultural materials and stone artefacts were variously carbonate encrusted and had to be treated to remove the carbonate.

## Radiocarbon Dating

Radiocarbon age estimates were obtained on a variety of cultural materials, including charcoal, freshwater mussel shell and *Celtis* sp. seeds (Table 1).

Small fragments or comminuted charcoal were recovered from most XUs (Figure 5b), though at depth the charcoal did not occur within the context of definite cultural features, such as hearths. In view of sediment cracking, bioturbation and root activity, these small fragments were regarded as unreliable for dating. *Celtis* sp. seeds and freshwater mussel shell also occurred in most XUs and, owing to their larger size, were considered less likely to have been displaced and, in the latter case, may be linked to human use of the cave (see below). However, the freshwater bivalves were once living within the limestone catchments and therefore have an unknown but potentially large freshwater reservoir effect (Keaveney and Reimer 2012; Lanting and van der Plicht 1998).

The endocarp of *Celtis* sp. seeds contains up to 70wt% carbonate (Wang et al. 1997). As seeds, they represent a single year of growth and derive their carbon from the atmosphere, and have been successfully used for dating elsewhere (Wang et al. 1997). Although they are regularly found in archaeological deposits in limestone caves, they are not likely to enter the cave as a result of human activity. Precisely how they enter the caves is unknown; they may be windblown, washed in by water or brought in by rodents, but if the latter they exhibit no gnawing damage.

### *Methods*

Like shells and coral, *Celtis* sp. is subject to diagenesis, primarily through recrystallisation which can lead to the incorporation of carbon of a different age. As the stable polymorph of carbonate, calcite will be deposited

| XU | Layers | Material | Laboratory Code | Radiocarbon Age (BP) | Calibrated Date cal. BP (95.4% Probability) | % Calcite |
|---|---|---|---|---|---|---|
| 1 | 1 | Charcoal and sand | ANU-10606 | 99.9±1.8 pMC | Modern | |
| 10 | 5–8 | Charcoal<br>*Celtis* inorganic | OZF-033<br>OZF-325 | 260±40<br>4790±40 | 441–75<br>5589–5326 | |
| 12 | 5–8 | *Celtis* inorganic | SANU-30229 | 5625±40 | 6436–6298 | <1 |
| 16 | 5–8 | *Celtis* inorganic | SANU-29413 | 9850±70 | 11,590–10,876 | |
| 18 | 5–8 | Freshwater mussel | OZD-163 | 12,650±190 | 15,540–14,140 | |
| 24 | 8–9b | *Celtis* inorganic | OZF-327 | 11,520±50 | 13,447–13,201 | |
| 29 | 8–11 | *Celtis* inorganic<br>Charcoal | OZF-324<br>OZF-359 | 13,870±70<br>14,100±300 | 17,014–16,442<br>17,870–16,249 | |
| 30 | 8–11 | Freshwater mussel | ANU-10784 | 10,486±179 | 12,715–11,709 | |
| 32 | 9a–11 | *Celtis* inorganic | SANU-29414 | 13,300±30 | 16,101–15,762 | 1.1±0.2 |
| 37 | 11 | *Celtis* inorganic | SANU-30227 | 14,020±60 | 17,208–16,658 | <1 |
| 38 | 11 | *Celtis* inorganic | SANU-29939 | 14,150 ±60 | 17,429–16,928 | 93.1±0.5 |
| 39 | 11 | Freshwater mussel | OZD-166 | 18,550±280 | 23,040–21,729 | |
| 49 | 11–12 | Freshwater mussel | OZD-167 | 21,450±270 | 26,202–25,143 | |
| 58 | 12–13 | Charcoal<br>Freshwater mussel | OZD-164<br>OZD-165 | 25,100±3590<br>24,900±570 | 46,660–23,955<br>30,372–27,846 | |
| 61 | 13 | Charcoal | D-AMS-001665 | 25,875±103 | 30,484–29,624 | |
| | | Freshwater mussel (nacre) | SANU-35003 | 27,400±160 | 31,467–31,010 | <1 |
| 64 | 13–14 | Freshwater mussel | SANU-35007 | 29,280±190 | 33,992–33,147 | |
| 67 | 13–14 | Freshwater mussel | SANU-35006 | 29,450±200 | 33,847–32,970 | |

**Table 1** Radiocarbon dates from CG3 calibrated against SHCal13 (Hogg et al. 2013) using OxCal v4.2 (Bronk Ramsey 2009a).

on recrystallisation. The carbonate of the endocarp is aragonite, meaning that recrystallisation, and therefore possible contamination, can be readily identified with x-ray diffraction (XRD). *Celtis* sp. seeds treated at The Australian National University (ANU) (i.e. laboratory codes prefixed SANU in Table 1) were subject to a 10% acid leach in 0.1M HCl at 80°C after removal of the surface with a scalpel. The cleaned carbonate was homogenised and divided into two aliquots. Approximately 8 mg was weighed into a blood collection vacutainer™, placed under vacuum and reacted with 0.5 mL 85% phosphoric acid. The $CO_2$ generated was cryogenically purified and graphitised over an iron catalyst with $H_2$ before measurement in a NEC SS-AMS (Fallon et al. 2010). The remaining material was used to screen for calcite. Approximately 10 mg of sample was crushed to a fine powder and suspended in an x-ray transparent glue on a plastic film. XRD analysis was performed in a STOE Stadi-P diffractometer operating at 30 mA and 40 kV. CoK radiation was used with a step size and time of 0.5° and 60 s between 24–60° 2 on the Bragg scale. Siroquant™ was used to quantify the calcite content, with a detection limit of ca 1% calcite. Of the five samples treated, three contained <1% calcite. One contained 5% calcite and was therefore not dated. A fifth sample (SANU-29939) contained more than 90% calcite, possibly suggesting the seed was burnt. Its date is not as reliable as the other dated seeds, though is similar in age to the sample from the XU above (SANU-30277). The pretreatment method used on the *Celtis* sp. seeds sent to ANSTO for dating is not known, though we do know that these seeds were not screened for calcite prior to analysis (i.e. laboratory codes prefixed OZF and OZD in Table 1).

Freshwater mussel shells dated at ANU (i.e. laboratory codes prefixed SANU) were treated using the same methods as the *Celtis* seeds. These shells naturally contain calcite and aragonite, but in one case (SANU-35003), nacre, made solely of aragonite, could be separated from the shell.

Charcoal and freshwater mussel shell samples were dated using conventional radiocarbon techniques at the ANU (i.e. laboratory codes prefixed ANU in Table 1). The charcoal/sand mixture of ANU-10606 was washed in 10% HCl prior to dating, whilst the surface of a freshwater mussel shell (ANU-10784), coated in a carbonate concretion, was ground with a dental drill and washed in water in an ultrasound bath.

Dates were calibrated in OxCal v.4.2 (Bronk Ramsey 2009a) against SHCal13 (Hogg et al. 2013). A Bayesian chronological model was constructed to calculate dates for the transition between stratigraphic layers and to identify and down-weight outliers (Bronk Ramsey 2009a, 2009b; Bronk Ramsey et al. 2010). The latter is particularly important where radiocarbon dates on a variety of materials have been dated using different methods, and where quality indicators, such as XRD, are not available. Terms relating specifically to OxCal are given in italics.

Numerous examples and explanations of the OxCal programme are available (e.g. Bayliss et al. 2007; Bronk Ramsey 2009a, 2009b; Higham et al. 2011). Briefly, the programme allows information about the relative chronology provided by stratigraphy to be combined with radiocarbon dates. The radiocarbon dates are grouped within *phases* (stratigraphic layers), and these *phases* are arranged within a *sequence*. Between each *phase* is a *boundary* that provides an estimate for the date of transition between the two *phases*.

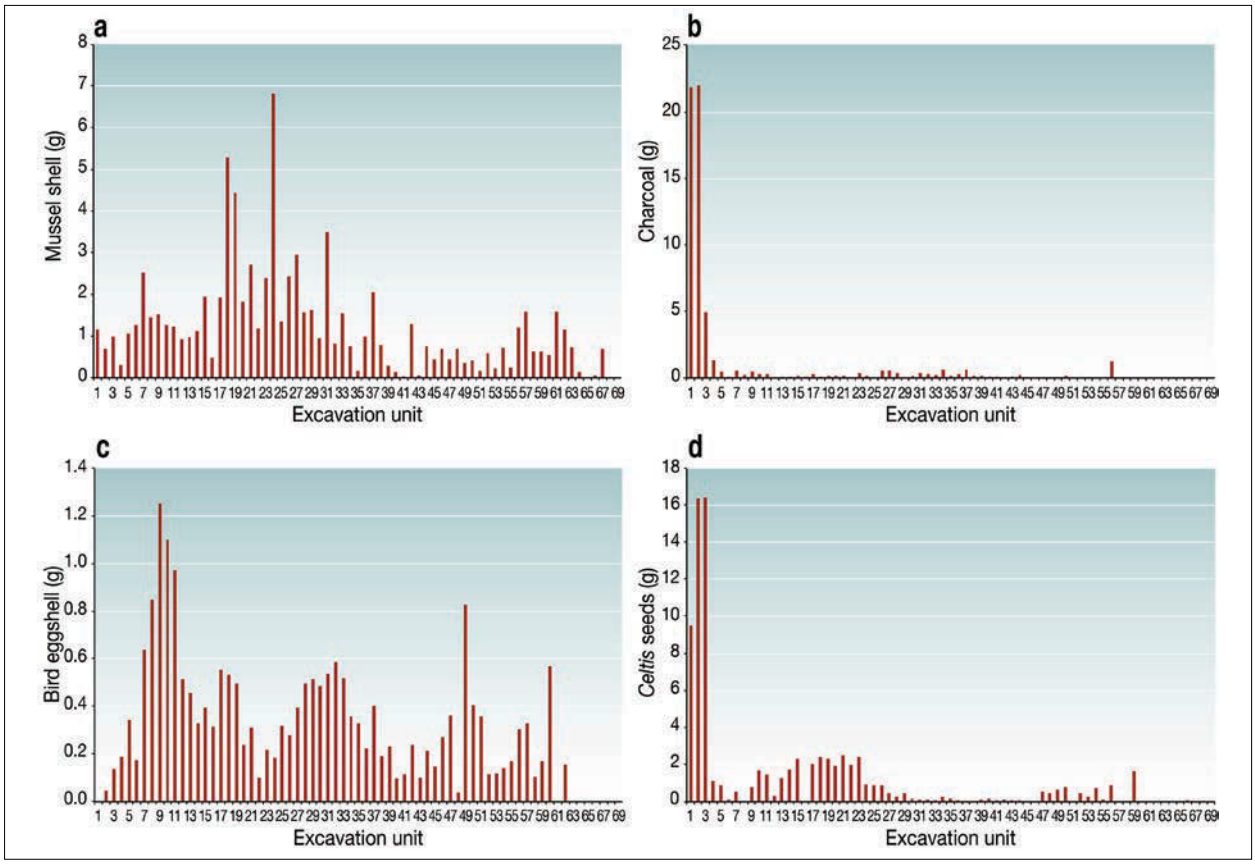


**Figure 5** Weights of recovered remains from CG3 by XU: (a) mussel shell; (b) charcoal; (c) bird eggshell; and (d) *Celtis* sp. seed.

It is these *boundaries*, or 'transition dates', that are plotted in Figure 6b and listed in Table 2. As noted above, at CG3 most XUs cut through several stratigraphic layers, so a series of overlapping *sequences* were cross-linked to a primary *sequence* containing all *boundaries* (Figures 6a and 6b). With the exception of those on mussel shells, the radiocarbon dates were assigned a prior outlier probability of 5% within the *General t-Type Outlier Model*, a flexible model which allows outliers to be either too young or too old (Bronk Ramsey 2009b). The mussel shells may have been affected by a freshwater reservoir effect, and have been assigned a higher prior probability of 50%, while one young charcoal date (OZF-033) has been excluded from the model. The prior outlier probability is revised during modelling, and a date's influence on the model is weighted according to the resulting outlier probability.

For a robust model, convergence should be above an arbitrary limit of ca 95% (Bronk Ramsey 2009a). Owing to the lack of stratigraphic constraints towards the top of the model, convergence of the final two *boundaries* (Transitions 7/5 and 5/4) is unacceptably low and these modelled date estimates should not be used (Table 2). Despite the variety of materials dated, the only samples found to have a much greater posterior probability of being an outlier than expected are OZD-166 and ANU-10784 (Figure 6c), both mussel shell. ANU-10784 is slightly young for its location, whilst OZD-166 is much older than expected. The significance of these dates has been down-weighted in the model, and they should not be used in discussions of the site chronology. Unfortunately, without XRD analysis, it is impossible to establish whether these outliers are the result of contamination, or whether the anomalously old sample may indicate that the shells are affected by a freshwater reservoir.

Whilst the imprecision of some *boundaries* in the Holocene limits their significance, others are more precise, particularly between Layers 8–12, where the highest number of dates have been obtained and XUs cross-cut fewer layers. The earliest occupation is found at the top of Layer 14 or, more likely, given the absence of any macroscopic or microscopic evidence of occupation in Layer 14, at the base of Layer 13. The earliest dates are on mussel shell in the spits cutting the top of Layer 14 and base of Layer 13. These place the first occupation after 34,440–31,340 cal. BP (at 68.2% probability, *boundary* 'Base'), although this may be a slight overestimation because the base of the model is heavily dependent on shell dates.

At the end of Layer 12 there appears to be a hiatus from 27,640–23,360 to 15,550–15,060 cal. BP (at 68.2% probability, *boundaries* 'End 12' and 'Start 11'), before deposition restarted. One sample, not identified as an outlier, OZD-167, falls within this gap. Unfortunately, this date is poorly constrained by the model, falling somewhere between the Transitions 13/12 and 11/9 *boundaries* (Sequence 4, Figure 6a). This means that the date could vary by 15,000 years and not be identified as an outlier by this model. The accuracy of the date is impossible to assess independently of the model as it is not accompanied by quality assurance data (e.g. XRD), and therefore this single date does not provide robust evidence for occupation during the otherwise apparent gap.

## The Stone Artefact Assemblage

A total of 2119 flaked lithic artefacts was recovered at CG3 from the 6 mm sieve fraction. The 3 mm fraction has not yet been analysed. The lowest lithic artefact was recovered from

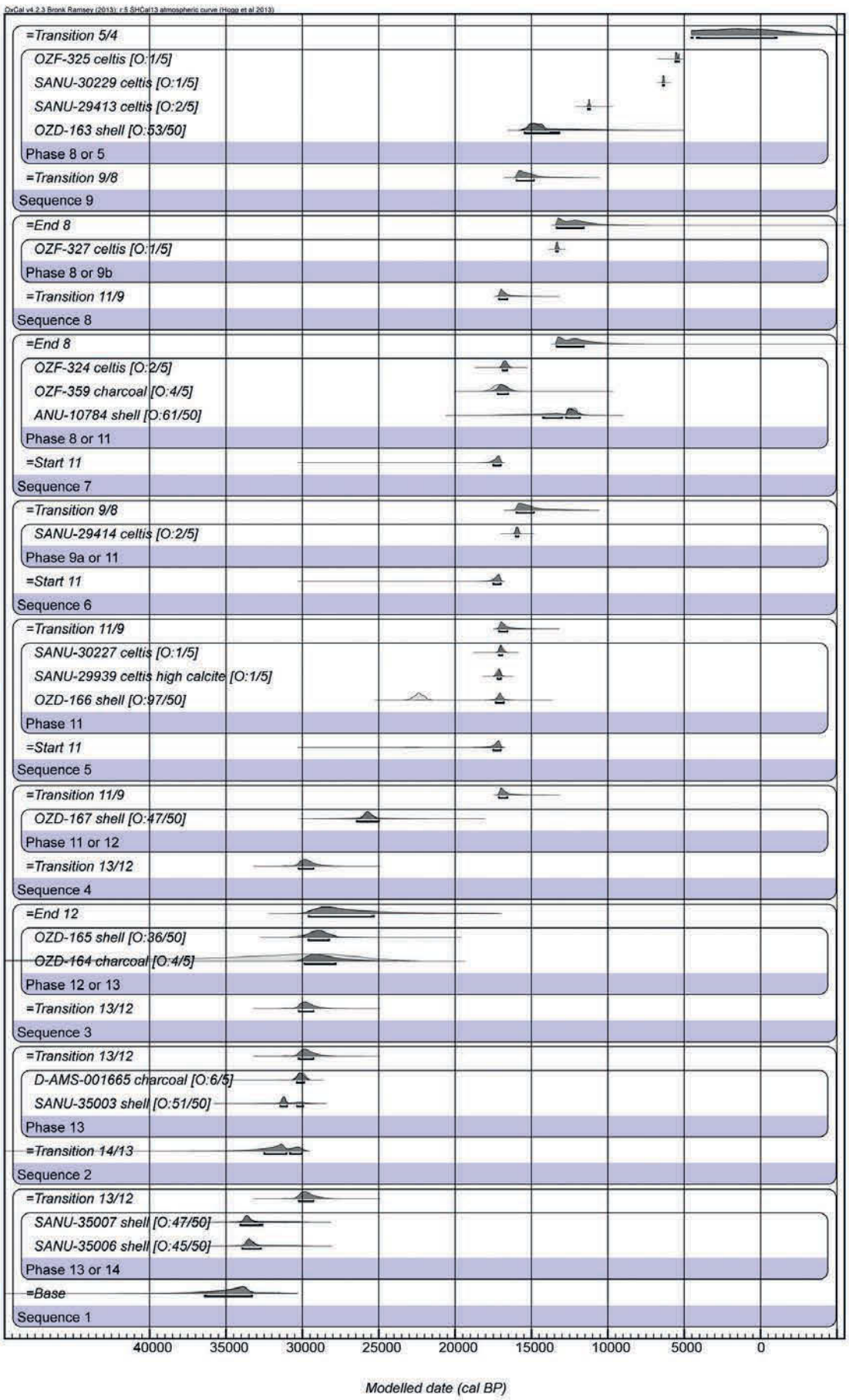


**Figure 6a** Bayesian model for the chronology of CG3. A series of single-*phase sequences* with radiocarbon dates, which have been cross-linked to the primary *sequence* in Figure 6b.

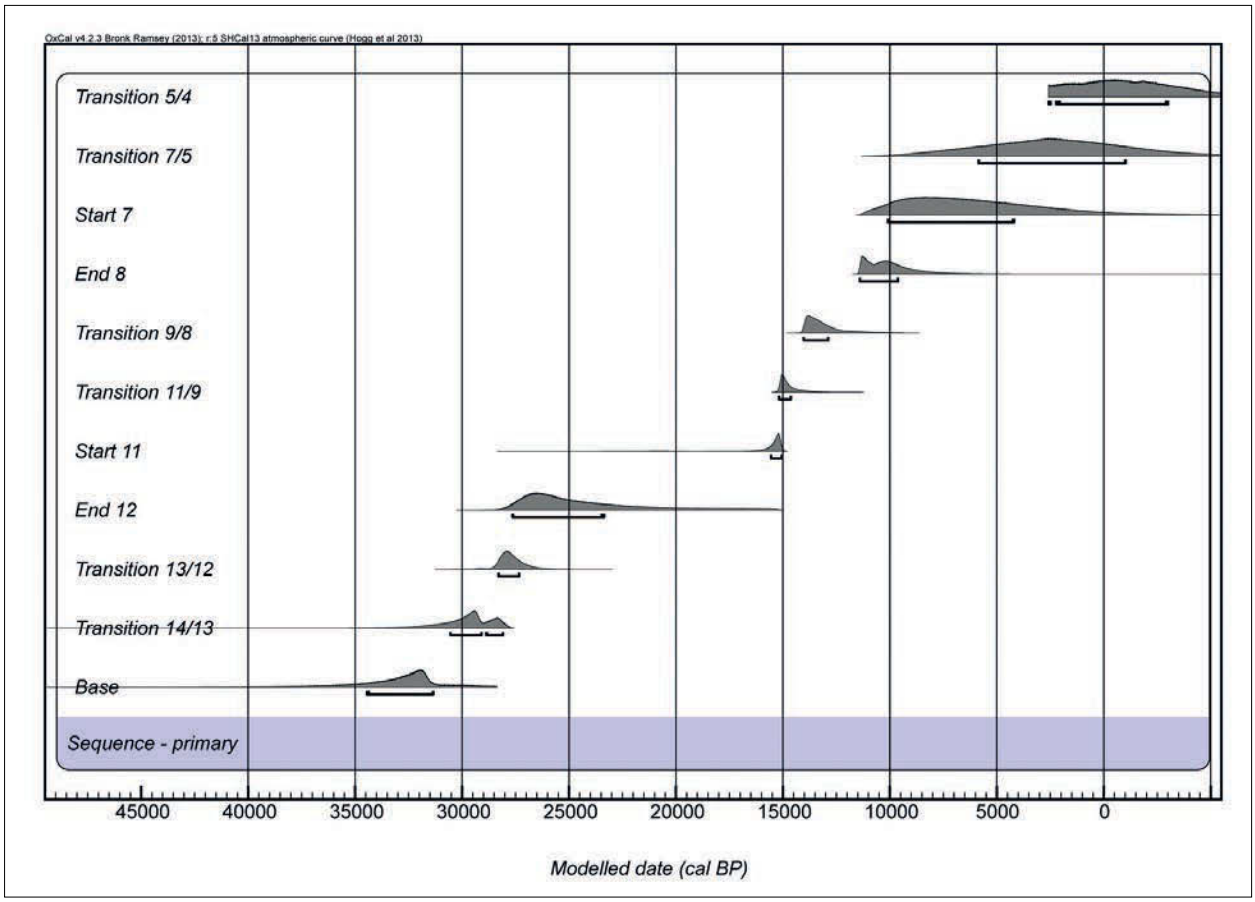


**Figure 6b** Summary of the 'transition dates' between layers. In Figures 6a and 6b the pale distribution represents the calibrated date, and the dark distribution the modelled date. The bar beneath each distribution denotes the 68.2% probability range.

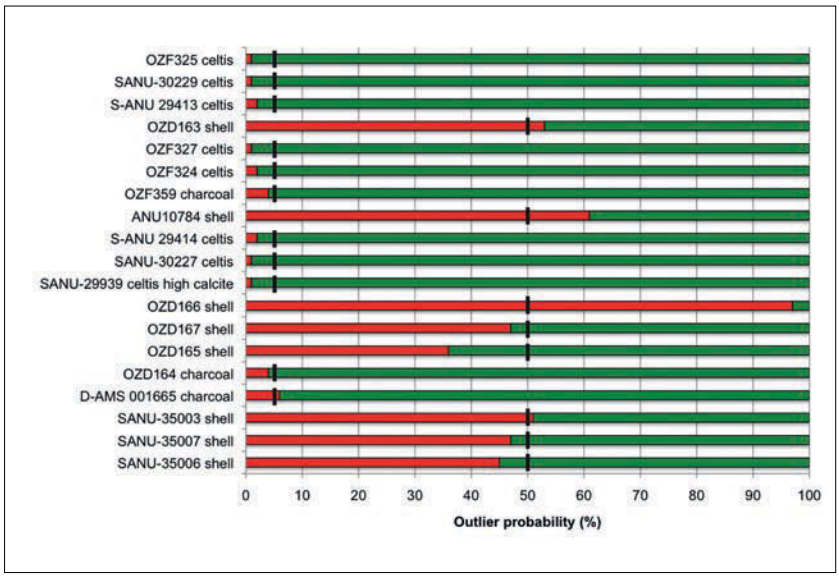


**Figure 6c** The probability the model found (the posterior probability) of each radiocarbon date being an outlier (red bar) compared to the prior likelihood of being an outlier (black line).

XU67 (Figure 7, Table 3). Figure 7 shows that the distribution of all stone artefacts and of the minimum number of flakes (MNF) correspond closely. The MNF is calculated by adding together the number of complete flakes, the higher number of proximal or distal fragments and a count of longitudinal fragments (after Hiscock 2002:254). This correlation demonstrates that lithic artefact accumulation is a real cultural trend and is not greatly affected by the tendency of quartz assemblages to have a greater relative frequency of flaked pieces.

Although significantly more sediment was removed per XU in the lower Pleistocene units, lithic artefact frequency is low (Figure 3). The majority of lithic artefacts occurred in XUs 4–10 (Figure 7), from the mid- to late Holocene. The timing of this peak in artefact discard appears to correspond with distinct technological changes and innovations in flaking strategies, such as is seen in other excavated assemblages from northern Australia (e.g. Clarkson 2008). In contrast to the CG3 assemblage, in the Victoria River region Clarkson reported two distinct peaks in artefact discard from excavations, one in the early Holocene and another in the late Holocene. The CG3 deposit records only one peak in the mid- to late Holocene.

The dominant raw material throughout the CG3 assemblage, accounting for >85% of lithic artefacts, is high quality translucent crystal quartz in the form of crystals and waterworn pebbles (Figure 8). Crystal quartz is occasionally found in formed crystals in the limestone, but can be more readily acquired from gullies and creeks where it has eroded from the conglomerate deposits of the Napier Ranges. The

| *Boundary* Between Layers | Modelled Date (cal. BP, 68.2% Probability) | | Modelled Date (cal. BP, 95.4% Probability) | | Convergence (%) |
|---|---|---|---|---|---|
| | From | To | From | To | |
| Transition 5/4 | 2578 | -3002 | … | -7869 | 35.5 |
| Transition 7/5 | 5857 | -1027 | 9187 | -4636 | 79.6 |
| Start 7 | 10,094 | 4189 | 11,163 | -30 | 96.0 |
| End 8 | 11,399 | 9622 | 11,482 | 7343 | 96.8 |
| Transition 9/8 | 14,030 | 12,885 | 14,142 | 10,771 | 99.1 |
| Transition 11/9 | 15,177 | 14,628 | 15,276 | 13,550 | 98.9 |
| Start 11 | 15,552 | 15,058 | 21,631 | 14,886 | 98.4 |
| End 12 | 27,641 | 23,359 | 28,068 | 17,232 | 97.2 |
| Transition 13/12 | 28,293 | 27,326 | 29,199 | 26,180 | 99.6 |
| Transition 14/13 | 30,537 | 28,088 | 32,536 | 27,796 | 90.8 |
| Base | 34,443 | 31,343 | 38,151 | 28,734 | 90.6 |

**Table 2** Probability distributions of the *boundaries* between stratigraphic layers modelled in Figure 6.

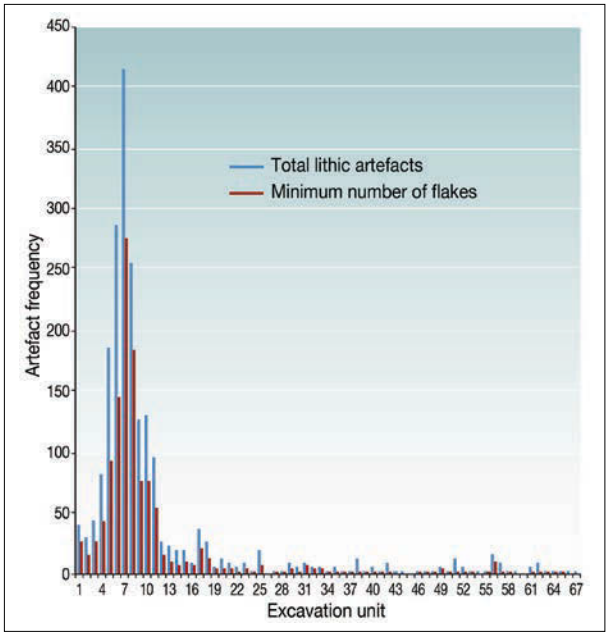


**Figure 7** Lithic artefact frequency and minimum number of flakes by XU.

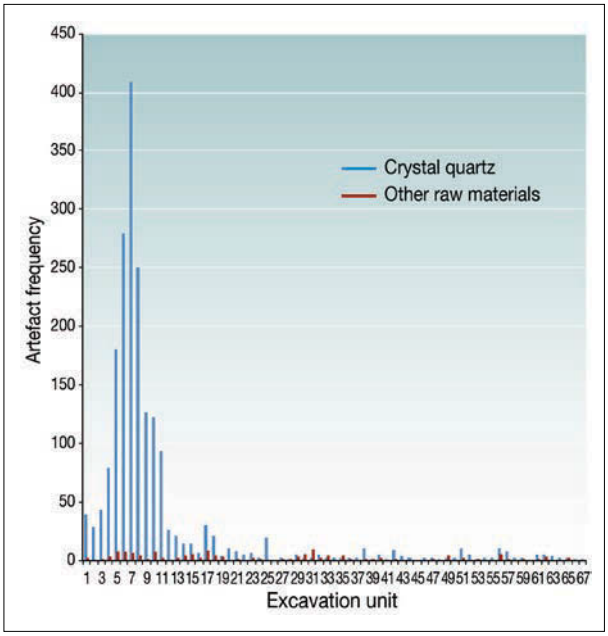


**Figure 8** Crystal quartz and other raw materials by XU.

Lennard River gravels contain a consistent component of crystal quartz waterworn pebbles; however, only occasionally are they of the same high quality crystal quartz discarded at CG3 (2008:Figures 13.9 and 13.10). The cortex of cores and flakes indicate focused exploitation of formed crystals and waterworn cobbles and only occasional use of white vein quartz, which is locally abundant but substantially lower in quality. Vast sheets of rounded quartzite cobbles and pebbles are found within 5 km of the site and occur in conglomerate bands within the CG3 complex. Two volcanic outcrops also occur within 10 km southeast of the site, and the limestone conglomerate of the Napier Range has similar volcanic inclusions. The low frequency of chert and chalcedony artefacts, together with the dominance of crystal quartz, suggests that people generally avoided utilisation of locally abundant, poor quality material in favour of higher quality materials that were either exotic or far less abundant.

After the early to mid-Holocene, flakes at CG3 gradually became more elongate, with marginal angles (the expanding or contracting of flake margins) approaching or exceeding 0 (ANOVA df = 855, f = 1.829, p = 0.0001). This trend is illustrated in Figure 9 and shows that, above XU16, there is a tendency for flakes to be more elongate, with either parallel or contracting margins. Flake mass relative to cutting edge (cf. Mackay 2008) also becomes gradually more standardised during this period (ANOVA df = 831, f = 1.166, p = 0.007). This is likely an indication of greater effort to control flake production, probably deriving from a combined need to maximise the economic utility of core and flake mass, as well as produce suitable blanks for point production.

The lowest bifacially flaked 'point' is made on hornfels and occurred in XU9, with three other bifacial points in XU8 (Figure 10). Five unifacially retouched points were also recovered above XU8. All nine points appear to be made on elongate flakes and none exhibit marginal pressure flaking (cf. Akerman and Bindon 1995:89).

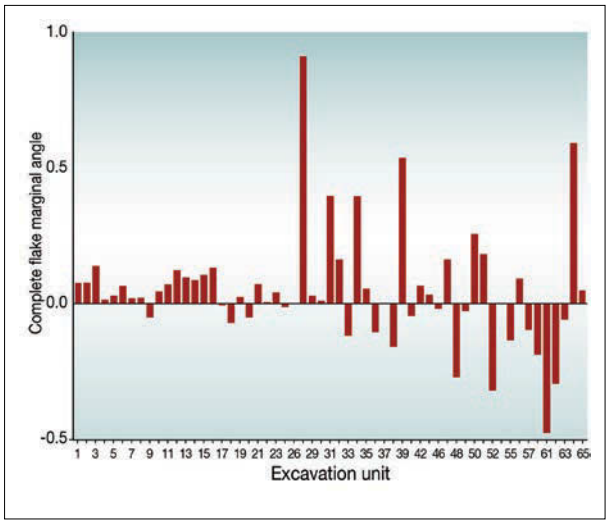


**Figure 9** Mean complete flake marginal angle by XU.

Retouched artefacts (n=74) are found in low frequency throughout the deposit and do not show any significant changes in the amount of retouch through time, as gauged by the Index of Invasiveness (Clarkson 2002) (ANOVA df = 25, f = 1.438, p = 0.158) and the Geometric Index of Unifacial Reduction (Kuhn 1990; see Hiscock and Clarkson 2005) (ANOVA df = 31, f = 1.438, p = 0.991). With the exception of points, these retouched artefacts are made on a wide range of flakes and exhibit marginal retouch mostly on one face. There is no correlation between the platform area of retouched flakes and non-retouched flakes (ANOVA df = 23, f = 0.582, p = 0.910), which suggests that blank morphologies come from the entire range of flakes produced, as represented in the 6 mm sieve fraction.

Cores (n=56) occur throughout the deposit and also suggest that reduction levels were generally greater in the Holocene. The number of core rotations, as an indication of the degree of reduction (Clarkson and O'Connor 2006:174), shows a significant correlation with depth (ANOVA df = 25, f = 1.908, p = 0.046). Cores with more than two rotations are mostly found in the Holocene levels.

XUs 62 and 65 contained edge-ground flakes made on a fine grained volcanic material of a basaltic type (Figures 11 and 12). Both were recovered below XU61, which produced a calibrated age range of 30,484–29,624 cal. BP, while XUs 63 and 67 have overlapping age ranges of 33,992–33,147 cal. BP and 33,847–32,970 cal. BP (Table 1).

Table 4 lists metric values of size and shape for the two edge-ground flakes. Cemented carbonate is attached to the surface of both and, in order to preserve any possible surface residues, has not been removed. The platforms of both exhibit ground surfaces, with visible striations on the polished surfaces. The flakes were therefore most likely removed from the ground margin of an axe and were not modified after their detachment. The nearby site of Carpenters Gap 1 (O'Connor 1995), about 2 km to the west, contains grinding grooves in sandstone beds with widths that are equivalent to a complete axe found on the surface of the CG3 overhang. These sandstone outcrops are sparely distributed in the Napier Range and are likely foci for edge-ground axe manufacture and maintenance. An additional edge-ground flake was recovered from XU10, seemingly made on the same fine grained volcanic material as the two Pleistocene flakes.

## Organic Materials

The upper XUs of CG3 contain the greatest quantities of macrobotanics, including charcoal and *Celtis* sp. seeds (Figure 5 and Table 3).

The distribution of *Celtis* sp. seeds throughout the deposit is not correlated with that of the stone artefacts or other material of definite anthropogenic origin. As such, we suggest these seeds more likely reflect the changing vegetation conditions through time in the immediate environment outside the cave (Figure 5). *Celtis* sp. seeds occur in XUs 59–47, decline dramatically during the Last Glacial Maximum (LGM), then increase from the terminal Pleistocene after about 13,000 years BP. XUs 1–3 contain the most *Celtis* sp. seeds, as well as abundant charcoal, the better preservation in these spits no doubt due to their more recent deposition.

The freshwater mussel in CG3 is identified as *Lortiella froggatti* (Iredale 1934), which is the only species found in the Kimberley. They were most likely collected from the adjacent Lennard River. Mussel shell was found in almost all XUs to the base of the site, including within the LGM units (Figure 5). There is a marked decrease in mussel shell in XUs 41–39, suggesting that the freshwater pools in the Lennard shrank or dried completely at times.

Pit A also included some marine shells, including two fragments of baler (*Melo* sp.) in XUs 4 and 14, and two small segments of scaphopod in XUs 12 and 14. XU12 dates to 6436–6298 cal. BP. The scaphopod segment from XU14 is bracketed by this date and another from XU16 of 11,590–10,876 cal. BP, suggesting it is of early Holocene age. The scaphopod shells were probably worn strung as beads, or as hair adornments. The baler shell fragment in XU4 has possible evidence for abrasion along part of the margin. Based on their distance inland, the baler shell finds are presumed to be the remnants of high value goods reduced through use and breakage and eventually discarded.

Small quantities of bones from large to medium-sized macropods were recovered from the Holocene units. Below this the majority of the bones were from small fauna and were likely derived from bird roosts above Pit A (see below). Unfortunately, during a pretreatment to remove carbonate encrustations from the bone from the 1993 excavation the wrong acid treatment was used and the bone was dissolved or badly damaged. No identifications could be made, or reliable weights obtained, on the fragments remaining. Thus no comparison was possible with the fauna excavated during the 2012 field season and this category of find has not been quantified.

Small fragments of bird eggshell were also recovered but have not been further identified. As noted above, in the lower part of Pit A much of the bone is thought to derive from a bird roost overlying the test pit, and thus the eggshell may not have an anthropogenic origin.

## Discussion and Conclusions

CG3 has evidence for intermittent occupation from 34,440–31,340 cal. BP through to the historic period. First habitation appears to coincide with the top of Layer 14, or more likely the base of Layer 13, with XUs 68–70 being culturally sterile. Scuffage and disturbance by people or animals in the upper shelter may have resulted in some cultural

| XU | Number of Lithic Artefacts | Mussel Shell (g) | Charcoal (g) | Bird Eggshell (g) | *Celtis* sp. Seed (g) | Sediment Volume (L) |
|---|---|---|---|---|---|---|
| 1 | 41 | 1.18 | 22.57 | 0 | 9.69 | 11.5 |
| 2 | 29 | 0.71 | 22.70 | 0.05 | 16.65 | 12.0 |
| 3 | 44 | 1.00 | 5.07 | 0.14 | 16.70 | 15.5 |
| 4 | 82 | 0.31 | 1.41 | 0.20 | 1.15 | 21.0 |
| 5 | 187 | 1.06 | 0.52 | 0.36 | 0.90 | 21.0 |
| 6 | 283 | 1.28 | 0.11 | 0.18 | 0.13 | 20.0 |
| 7 | 414 | 2.55 | 0.59 | 0.66 | 0.55 | 24.0 |
| 8 | 251 | 1.47 | 0.26 | 0.88 | 0 | 25.0 |
| 9 | 123 | 1.55 | 0.49 | 1.30 | 0.78 | 20.0 |
| 10 | 129 | 1.29 | 0.31 | 1.14 | 1.73 | 25.0 |
| 11 | 90 | 1.23 | 0.31 | 1.01 | 1.48 | 30.5 |
| 12 | 26 | 0.94 | 0 | 0.53 | 0.30 | 17.0 |
| 13 | 22 | 0.97 | 0.02 | 0.47 | 1.28 | 19.0 |
| 14 | 17 | 1.13 | 0.02 | 0.34 | 1.77 | 25.5 |
| 15 | 20 | 1.98 | 0.13 | 0.41 | 2.34 | 29.0 |
| 16 | 8 | 0.49 | 0.03 | 0.33 | 0 | 18.5 |
| 17 | 36 | 1.95 | 0.29 | 0.58 | 2.04 | 27.5 |
| 18 | 21 | 5.36 | 0.06 | 0.55 | 2.44 | 30.0 |
| 19 | 7 | 4.49 | 0.15 | 0.51 | 2.36 | 18.5 |
| 20 | 11 | 1.85 | 0.17 | 0.25 | 1.97 | 21.0 |
| 21 | 8 | 2.75 | 0.17 | 0.32 | 2.52 | 23.5 |
| 22 | 5 | 1.19 | 0 | 0.10 | 2.01 | 15.5 |
| 23 | 7 | 2.43 | 0.37 | 0.22 | 2.43 | 19.5 |
| 24 | 4 | 6.91 | 0.13 | 0.19 | 0.92 | 15.0 |
| 25 | 10 | 1.37 | 0 | 0.33 | 0.92 | 23.5 |
| 26 | 0 | 2.47 | 0.55 | 0.29 | 0.90 | 19.5 |
| 27 | 4 | 2.99 | 0.58 | 0.41 | 0.46 | 23.0 |
| 28 | 2 | 1.58 | 0.36 | 0.51 | 0.27 | 30.0 |
| 29 | 7 | 1.65 | 0 | 0.53 | 0.45 | 15.5 |
| 30 | 7 | 0.96 | 0.13 | 0.50 | 0.16 | 20.0 |
| 31 | 9 | 3.54 | 0.37 | 0.56 | 0.11 | 25.5 |
| 32 | 7 | 0.83 | 0.32 | 0.61 | 0.10 | 22.0 |
| 33 | 7 | 1.57 | 0.24 | 0.54 | 0.03 | 20.5 |
| 34 | 3 | 0.76 | 0.63 | 0.37 | 0.25 | 18.5 |
| 35 | 5 | 0.16 | 0.14 | 0.34 | 0.16 | 21.0 |
| 36 | 3 | 1.00 | 0.30 | 0.23 | 0.04 | 18.5 |
| 37 | 2 | 2.09 | 0.63 | 0.42 | 0 | 21.5 |
| 38 | 8 | 0.79 | 0.17 | 0.20 | 0 | 28.5 |
| 39 | 2 | 0.29 | 0.16 | 0.24 | 0.10 | 19.5 |
| 40 | 6 | 0.15 | 0.12 | 0.10 | 0.14 | 17.5 |
| 41 | 1 | 0.01 | 0.06 | 0.12 | 0.04 | 11.5 |
| 42 | 10 | 1.31 | 0 | 0.25 | 0.14 | 25.5 |
| 43 | 3 | 0.06 | 0.08 | 0.10 | 0.02 | 17.0 |
| 44 | 1 | 0.77 | 0.26 | 0.22 | 0.06 | 25.0 |
| 45 | 0 | 0.45 | 0 | 0.15 | 0 | 22.0 |
| 46 | 3 | 0.70 | 0 | 0.28 | 0 | 41.5 |
| 47 | 4 | 0.44 | 0 | 0.38 | 0.54 | 54.0 |

**Table 3** Stone artefact numbers, weights of organic material and sediment volumes. Continued overleaf.

| XU | Number of Lithic Artefacts | Mussel Shell (g) | Charcoal (g) | Bird Eggshell (g) | *Celtis* sp. Seed (g) | Sediment Volume (L) |
|---|---|---|---|---|---|---|
| 48 | 1 | 0.70 | 0 | 0.04 | 0.46 | 47.0 |
| 49 | 7 | 0.35 | 0 | 0.86 | 0.63 | 67.5 |
| 50 | 2 | 0.41 | 0.16 | 0.42 | 0.78 | 62.0 |
| 51 | 2 | 0.16 | 0 | 0.37 | 0 | 56.0 |
| 52 | 4 | 0.59 | 0 | 0.12 | 0.48 | 68.5 |
| 53 | 2 | 0.23 | 0 | 0.12 | 0.28 | 62.5 |
| 54 | 1 | 0.72 | 0 | 0.14 | 0.77 | 58.5 |
| 55 | 3 | 0.25 | 0 | 0.18 | 0.13 | 57.5 |
| 56 | 12 | 1.22 | 1.30 | 0.32 | 0.90 | 85.0 |
| 57 | 7 | 1.60 | 0 | 0.34 | 0 | 65.5 |
| 58 | 2 | 0.63 | 0 | 0.11 | 0 | 67.0 |
| 59 | 2 | 0.63 | 0 | 0.18 | 1.69 | 56.5 |
| 60 | 0 | 0.55 | 0 | 0.59 | 0 | 50.5 |
| 61 | 6 | 1.61 | 0 | 0 | 0 | 52.0 |
| 62 | 8 | 1.17 | 0 | 0.16 | 0 | 48.5 |
| 63 | 4 | 0.75 | 0 | 0 | 0 | 42.1 |
| 64 | 3 | 0.13 | 0 | 0 | 0 | 34.3 |
| 65 | 4 | 0 | 0 | 0 | 0 | 26.0 |
| 66 | 1 | 0.05 | 0 | 0 | 0.07 | 40.5 |
| 67 | 1 | 0.69 | 0 | 0 | 0 | 41.5 |
| 68 | 0 | 0 | 0 | 0 | 0 | 71.7 |
| 69 | 0 | 0 | 0 | 0 | 0 | 47.5 |

**Table 3 continued** Stone artefact numbers, weights of organic material and sediment volumes.

material displaced into the lower cave; however, the small quartz flakes recovered in most XUs indicate that artefact maintenance and manufacture was taking place within the cave itself. In an earlier publication (O'Connor and Veth 2006:35), it was suggested that stone artefacts at CG3 might be more abundant during the LGM than at nearby CG1, owing to the fact that CG3 is located close to the Lennard River. However, detailed analysis resulted in the elimination as artefacts of many pieces of stone collected during the excavation. It is clear from Table 4 that artefact numbers are uniformly low from first occupation in XU67 through to the terminal Pleistocene.

There are no radiocarbon dates for the period 21,000–18,000 cal. BP at CG3. The Bayesian model indicates an even longer break in occupation, between 27,640–23,360 to 15,550–15,060 cal. BP. In view of the location of CG3 proximal to the Lennard River, evidence for habitation is surprisingly sparse during the terminal Pleistocene, and it is possible that the Lennard ceased to flow or dried completely at times during the LGM. There are also indications of extreme climate variability throughout this phase which, coupled with aridity, may have affected people's ability to occupy the region (Dennison et al. 2013). Nearby CG1 had extremely sparse evidence for occupation during this time period, while Riwi, ca 200 km to the southeast of CG3, contained no evidence for occupation between ca 34,000 cal. BP and 6000 cal. BP (Balme 2000; McConnell and O'Connor 1999:26, 32–33). It has been suggested that, due to aridity, the landscape may have presented limited opportunities for expansion into the margins of the arid zone during the terminal Pleistocene (Hiscock and Wallis 2004; O'Connor and Veth 2006:36–37). Riwi was re-excavated in 2013, with a larger area excavated, much finer XUs, and dating samples collected in situ. The results of this work are pending and may alter what is currently known of the timing of occupation on the northern edge of the Great Sandy Desert.

Although low numbers of artefacts were discarded during the Pleistocene at CG3, the presence of flakes from edge-ground axes indicates that maintenance of tools was carried out within the cave during the earliest period of occupation about 34,000 years ago. These artefacts add to the known sample of Pleistocene edge-ground axe technology from northern Australia. The fact that flakes from axes are represented in assemblages with very low numbers of artefacts overall suggests that these tools formed an important component of the lithic repertoire following initial settlement across northern Australia (see Davidson and Noble 1992:49, Table 1; Geneste et al. 2010:4). We have suggested elsewhere that, like their Holocene counterparts, Pleistocene axes and hatchets were likely multipurpose tools used for a variety of extraction activities (Balme and O'Connor 2014). While they required hafting and the working edge required intense curation; the durability, long use-life and functional flexibility of these tools would have made them particularly useful in colonising situations where raw materials, resources and stone supply zones could not be anticipated.

In common with most Australian sites, evidence for occupation at CG3 increases sharply in the mid- to late Holocene. The timing of this change is poorly resolved at CG3 due to the small number of dates covering the upper

| Artefact ID Number | Length (mm) | Width (mm) | Elongation (mm) | Thickness (mm) | External Platform Angle (°) | Mass (g) |
|---|---|---|---|---|---|---|
| XU-62 # 2105 | 36.3 | 52.8 | 0.69 | 10.4 | 90 | 23.6 |
| XU-65 # 2093 | 24.4 | 34.3 | 0.71 | 6.7 | 50 | 10.2 |

**Table 4** Measurements for Pleistocene edge-ground flakes from XUs 62 and 65.

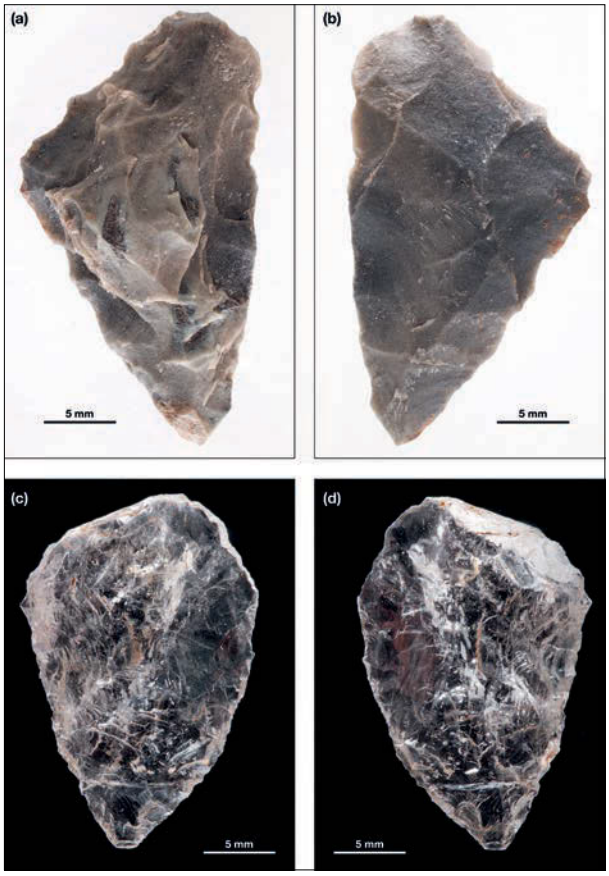


**Figure 10** Bifacial points from CG3: (a) hornfels bifacial point recovered from XU9 showing likely dorsal face with invasive flaking scars; (b) likely ventral surface of the same hornfels bifacial point showing scars initiated from dorsal surface are truncated by proceeding scars initiated from ventral surface; (c) crystal quartz bifacial point recovered from XU8 showing dorsal surface with invasive retouch scars; and (d) ventral surface of same crystal quartz bifacial point showing invasive retouch scars and a marginal break on the proximal end.

part of the sequence; however, in view of the sediment cracking and bioturbation in the upper XUs, additional dating is unlikely to clarify the situation. The evidence for increased site use is not a taphonomic effect, as it is most evident in the frequency of stone artefacts. It is also clearly unrelated to the volume of sediment excavated, as volumes removed were much greater in the lower XUs than in those dated to the mid- to late Holocene. Interestingly, the increase in occupation from the mid-Holocene at CG3 coincides with Holocene reoccupation at Riwi (Balme 2000), perhaps reflecting a demographic increase in the southern Kimberley followed by population expansion into the northern margins of the arid zone. Williams (2013:8) has recently argued that time-series modelling of all available radiocarbon dates from all Australian archaeological sites demonstrates population increase on a continent-wide basis in the mid- to late Holocene.

The presence of freshwater mussel shell in almost all XUs indicates that the people at CG3 exploited a nearby freshwater source, probably the Lennard River, as it is

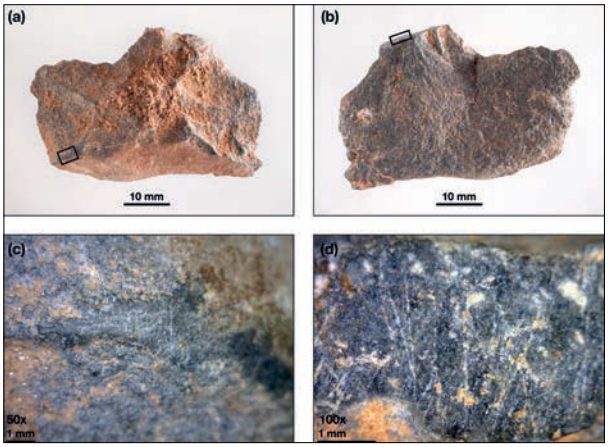


**Figure 11** Pleistocene ground-edge flake recovered from XU62: (a) dorsal surface; (b) ventral surface; (c) 50x magnification of dorsal ridge on left distal portion of flake showing striations over polished surface; and (d) 100x magnification of platform surface showing multiple intersecting striations over polished surface.

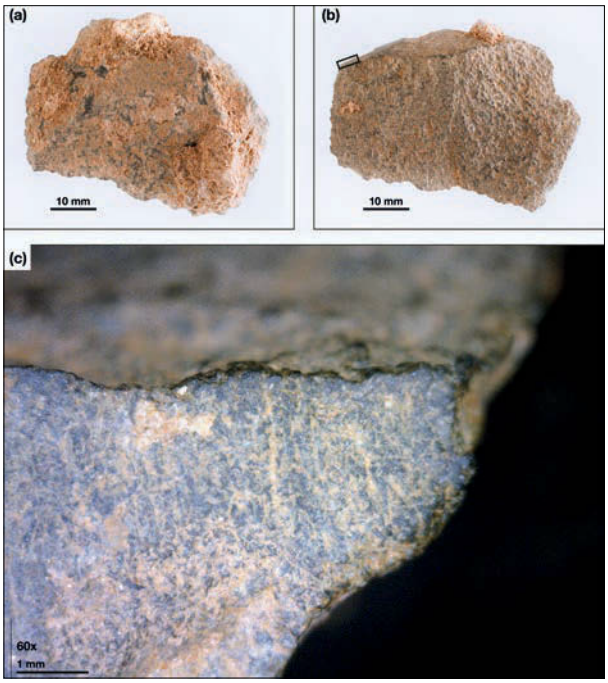


**Figure 12** Pleistocene ground-edge flake recovered from XU65: (a) dorsal surface; (b) ventral surface, ground edge surface is located on platform; and (c) 60x magnification of edge-ground platform surface showing several striations over polished surface.

unlikely that these bivalves would have been transported any great distance. The marked decrease in freshwater mussel during the LGM no doubt reflects the effects of aridity and retraction of the freshwater pools where this resource was procured. In contrast, the scaphopod and baler shell must have derived from the coast over 200 km to the west and been transported inland along trade/exchange networks. All of the marine shell at CG3 occurs in Holocene units, with three of the four pieces in XUs 12 and 14 dated between

about 6000 cal. BP and the early Holocene. Scaphopod beads have been recovered from CG1 and other sites in the southern inland Kimberley and as far east as Riwi, where they were in Pleistocene-aged deposits (Balme 2000; Balme and Morse 2006). The widespread archaeological distribution of such beads in the inland Kimberley suggests they were a reasonably common item of personal decoration, however, they are not documented in Museum collections as ethnographic items from this far inland. The presence of baler shell pieces in inland locations at approximately 32,000 cal. BP at Widgingarri Shelter 1 in the west Kimberley (O'Connor 1999:60, 121), and at ca 22,000 cal. BP at the Silver Dollar site, Shark Bay, in the Pilbara (Bowdler 1990), established an early archaeological context for use of baler shell in northwest Australia and its movement at least 70–100 km inland. In historic times, baler shells were traded many hundreds of kilometres from coastal regions into the desert where they were used in ceremony (Smith and Veth 2004). As they moved inland they gained value, changed meaning (Mulvaney 1976), and reduced in size.

## Acknowledgements

The authors would like to acknowledge the assistance of Bunuba Aboriginal Corporation and the Bunuba Rangers. In particular, June Oscar was a constant support during our fieldwork. DEC WA provided logistical support during our 2012 field season in the Windjana Gorge National Park. The fieldwork for this paper was funded by the ARC Linkage Grant LP100200415, with contributions from the Kimberley Foundation Australia and the Department of Sustainability, Water, Populations and Communities.

## References

Akerman, K. and P. Bindon 1995 Dentate and related stone biface points from northern Australia. *The Beagle, Records of the Museums and Art Galleries of the Northern Territory* 80:799–811.

Balme, J. 2000 Excavations revealing 40,000 years of occupation at Mimbi Caves, south central Kimberley, Western Australia. *Australian Archaeology* 51:1–5.

Balme, J. and K. Morse 2006 Shell beads and social behaviour in Pleistocene Australia. *Antiquity* 51:1–5.

Balme, J. and S. O'Connor 2014 Early modern humans in Island Southeast Asia and Sahul: Adaptive and creative societies with simple lithic industries. In R. Dennell and M. Porr (eds), *East of Africa: Southern Asia, Australia and Human Origins,* pp.164–174. Cambridge: Cambridge University Press.

Bayliss, A., C. Bronk Ramsey, J. van der Plicht and A. Whittle 2007 Bradshaw and Bayes: Towards a timetable for the Neolithic. *Cambridge Archaeological Journal* 17(1):1–28.

Bowdler, S. 1990 The Silver Dollar site, Shark Bay: An interim report. *Australian Aboriginal Studies* 1990(2):60–63.

Bronk Ramsey, C. 2009a Bayesian analysis of radiocarbon dates. *Radiocarbon* 51(1):337–360.

Bronk Ramsey, C. 2009b Dealing with outliers and offsets in radiocarbon dating. *Radiocarbon* 51(3):1023–1045.

Bronk Ramsey, C., M. Dee, S. Lee, T. Nakagawa and R. Staff 2010 Developments in the calibration and modelling of radiocarbon dates. *Radiocarbon* 52(3):953–961.

Clarkson, C. 2002 An index of invasiveness for the measurement of unifacial and bifacial retouch: A theoretical, experimental and archaeological verification. *Journal of Archaeological Science* 29(1):65–75.

Clarkson, C. 2008 Changing reduction intensity, settlement and subsistence in Wardaman Country, northern Australia. In W. Andrefsky (ed.), *Lithic Technology*, pp.286–316. New York: Cambridge University Press.

Clarkson, C. and S. O'Connor 2006 An introduction to stone artifact analysis. In J. Balme and A. Paterson (eds), *Archaeology in Practice: A Student Guide to Archaeological Analyses,* pp.159–206. Malden, MA: Blackwell Publishing.

Davidson, I. and W. Noble 1992 Why the first colonisation of the Australian region is the earliest evidence of modern human behavior. *Archaeology in Oceania* 27(3):113–119.

Dennison, R.F., K-H. Wyrwoll, Y. Asmerom, V.J. Polyak, W.F. Humphreys, J. Cugley, D. Woods, Z. LaPointe, J. Peota and E. Greaves 2013 North Atlantic forcing of millennial-scale Indo-Australian monsoon dynamics during the last glacial period. *Quaternary Science Reviews* 72:159–168.

Fallon, S., L. Fifield and J. Chappell 2010 The next chapter in radiocarbon dating at The Australian National University: Status report on the single stage AMS. *Nuclear Instruments and Methods in Physics Research B* 268(8):298–901.

Geneste, J-M., B. David, H. Plisson, C. Clarkson, J-J. Delannoy, F. Petchey and R. Whear 2010 Earliest evidence for ground-edge axes: 35,400±410 cal. BP from Jawoyn Country, Arnhem Land. *Australian Archaeology* 71:66–69.

Higham, T.F.G., R.M. Jacobi, L. Basell, C. Bronk Ramsey, L. Chiotti and R. Nespoulet 2011 Precision dating of the Palaeolithic: A new radiocarbon chronology for the Abri Pataud (France), a key Aurignacian sequence. *Journal of Human Evolution* 61(5):549–563.

Hiscock, P. 2002 Quantifying the size of artefact assemblages. *Journal of Archaeological Science* 29:251–258.

Hiscock, P. and C. Clarkson 2005 Measuring artefact reduction: An examination of Kuhn's geometric index of reduction. In C. Clarkson and L. Lamb (eds), *Lithics 'Down Under': Australian Perspectives on Lithic Reduction, Use and Classification*, pp.7–19. BAR International Series 1408. Oxford: Archaeopress.

Hiscock, P. and L. A. Wallis 2004 Pleistocene settlements of deserts from an Australian perspective. In P. Veth, M. Smith and P. Hiscock (eds), *Desert Peoples: Archaeological Perspectives*, pp.34–57. Oxford: Blackwell.

Hogg, A.G., Q. Hua, P.G. Blackwell, M. Niu, C.E. Buck, T.P. Guilderson, T.J. Heaton, J.G. Palmer, P.J. Reimer, R.W. Reimer, C.S.M. Turney and S.R.H. Zimmerman 2013 SHCal13 Southern Hemisphere calibration, 0–50,000 years cal. BP. *Radiocarbon* 55(4):1889–1903.

Iredale, T. 1934 The freshwater mussels of Australia. *Australian Zoologist* 8:57–78.

Kuhn, S. 1990 A geometric index of unifacial reduction for stone tools. *Journal of Archaeological Science* 17:585–593.

Lanting, J.N. and J. van der Plicht 1998 Reservoir effects and apparent 14C ages. *The Journal of Irish Archaeology* 9:151–165.

Mackay, A. 2008 A method for estimating edge length from flake dimensions: Use and implications for technological change in the southern African MSA. *Journal of Archaeological Science* 35(3):614–622.

McConnell, K. and S. O'Connor 1999 Carpenters Gap Shelter 1, a case for total recovery. In M-J. Mountain and D. Bowdery (eds), *Taphonomy: The Analysis of Processes from Phytoliths to Megafauna*, pp.23–34. Canberra: ANH Publications.

McCormac, F.G., A.G. Hogg, P.G. Blackwell, C.E. Buck, T.F.G. Higham and P.J. Reimer 2004 SHCal04 Southern Hemisphere calibration, 0–11.0 cal. kyr BP. *Radiocarbon* 46(3):1087–1092.

Mulvaney, D.J. 1976 'The chain of connection': The material evidence. In N. Peterson (ed.), *Tribes and Boundaries in Australia*, pp.72–94. Canberra: Australian Institute of Aboriginal Studies.

O'Connor, S. 1995 Carpenters Gap Rockshelter 1: 40,000 years of Aboriginal occupation in the Napier Range, Kimberley, WA. *Australian Archaeology* 40:58–59.

O'Connor, S. 1999 *30,000 Years of Aboriginal Occupation: Kimberley, North West Australia.* Terra Australis 14. Canberra: ANH Publications, The Australian National University.

O'Connor, S. and P. Veth 2006 Revisiting the past: Changing interpretations of Pleistocene settlement subsistence and demography in northern Australia. In I. Lilley (ed.), *Archaeology of Oceania, Australia and the Pacific Islands,* pp.31–47. Oxford: Blackwell Publishing.

Reimer, P.J., M.G.L. Baillie, E. Bard, A. Bayliss, J.W. Beck, P.G. Blackwell, C. Bronk Ramsey, C.E. Buck, G.S. Burr, R.L. Edwards, M. Friedrich, P.M. Grootes, T.P. Guilderson, I. Hajdas, T.J. Heaton, A.G. Hogg, K.A. Hughen, K.A. Kaiser, B. Kromer, F.G. McCormac, S.W. Manning, R.W. Reimer, D.A. Richards, J.R. Southon, S. Talamo, C.S.M. Turney, J. Van Der Plicht and C.E. Weyhenmeyer 2009 IntCal09 and Marine09 radiocarbon age calibration curves, 0–50,000 years cal. BP. *Radiocarbon* 59:1111–1150.

Smith, M.A. and P.M. Veth 2004 Radiocarbon dates for baler shell in the Great Sandy Desert. *Australian Archaeology* 58:37–38.

Wang, Y., A.H. Jahren and R. Amundson 1997 Potential for 14C dating of biogenic carbonate in hackberry (*Celtis*) endocarps. *Quaternary Research* 47(3):337–343.

Williams, A.N. 2013 A new population curve for prehistoric Australia. *Proceedings of the Royal Society B* 280 <http://dx.doi.org/10.1098/rspb.2013.0486>.